CRITICAL FIELDS IN A HEXAGONAL STRONTIUM FERRITE

D. G. SANNIKOV and T. M. PEREKALINA

Institute of Crystallography, Academy of Sciences, U.S.S.R.

Submitted August 28, 1968

Zh. Eksp. Teor. Fiz. 56, 730–735 (March, 1969)

The magnetic properties possessed by single crystals of the hexagonal ferrite $(Ba_{0.2}Sr_{0.8})_3Zn_2Fe_{24}O_{41}$ are investigated. Magnetization curves which exhibit the existence of critical fields are measured at different temperatures. The temperature dependences of the anisotropy constants are measured. Magnetization curves are calculated using the model of two magnetic sublattices with a weak exchange interaction, and are found to be in good agreement with experiment.

THE very diverse structures of hexagonal ferrites are accompanied by a diversity of their magnetic properties. In the present work we have investigated the magnetic properties (magnetization curves and anisotropy constants) of the hexagonal ferrite $(Ba_{0.2}Sr_{0.8})_3Zn_2Fe_{24}O_{41}$ (abbreviated to Sr_3Zn_2Z) and have discovered that critical magnetic fields exist at which the magnetic properties of this ferrite are changed. At the present time only very few additional substances associated with such critical fields are known. It is therefore useful to present the results obtained in our investigation of the magnetic properties exhibited by single crystals of Sr_3Zn_2Z.

1. The Sr_3Zn_2Z crystals were grown by spontaneous crystallization from a solution in a $NaFeO_2$ melt. An x-ray analysis yielded the unit cell parameters c = 52.26 Å and a = 5.87 Å. The strontium and zinc contents were determined with an x-ray microanalyzer.

A vibration magnetometer was used to measure the magnetization curves of the Sr_3Zn_2Z single crystals in the temperature range 77–650°K. Curve 1 in Fig. 1 was obtained for a magnetic field parallel to the c axis of crystal symmetry; curves 2–6 were obtained with the magnetic field in the basal plane.[1)] The respective temperatures corresponding to the curves are given. The existence of a critical field that is linearly dependent on temperature is clearly shown by curves 2–5 (the lower graph in Fig. 1). The slow rise exhibited by curves 2–6 in the region $H < H_{cr}$ is evidence of a "paraprocess." For very low fields $H < 0.5$ kOe the curves are unreliable because the demagnetizing field that was present could not be taken into account completely.

The torque method was used to investigate magnetic anisotropy in the same samples. It was found that above 230°K the direction of easy magnetization coincides with the c axis of Sr_3Zn_2Z crystals. Below 230°K the easy magnetization direction forms an angle α with the c axis and thus generates a cone of easy magnetization. The angle α increases as the temperature is reduced and has the value 23° at 77°K. The magnetic anisotropy energy of a hexagonal ferrite can be expressed by the equation

$$\Phi_k = -{}^1/_2 K_1 \cos^2\psi - {}^1/_4 K_2 \cos^4\psi, \qquad (1)$$

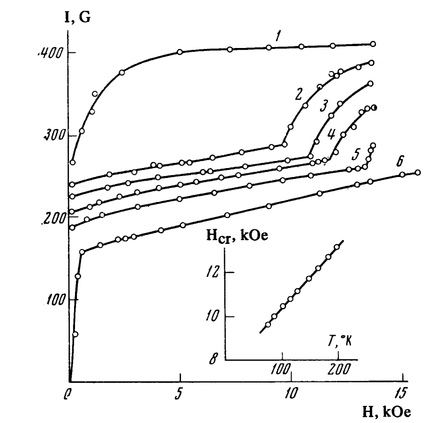

FIG. 1. Magnetization curves (magnetization I versus applied magnetic field H). For H∥c: 1 – T = 77°K; for H⊥c: 2 – T = 77°K, 3 – 125°K, 4 – 155°K, 5 – 205°K, 6 – 293°K.

where ψ is the angle between the magnetization vector I and the c axis. The anisotropy constants K_1 and K_2 are determined from experimental torque curves. Figure 2 shows the temperature dependences of K_1 and K_2.

2. The magnetic structure of ferrites is quite complex.[1] However, for a description of their magnetic properties it is often sufficient to consider the model of two magnetic sublattices characterized by the magnetic moment vectors **M** and **M′**;[2] this model is used in the present work. Then the thermodynamic potential for unit volume of an infinite hexagonal ferrite crystal is given by

$$\Phi = -{}^1/_2 K\cos^2\theta - {}^1/_2 K'\cos^2\theta' + K''\cos\theta\cos\theta' + K'''\sin\theta\sin\theta'\cos(\varphi-\varphi') + \varkappa \mathbf{MM'} - \mathbf{HM} - \mathbf{HM'}. \qquad (2)$$

Here the terms having the different K coefficients represent the magnetic anisotropy in the first perturbation approximation; θ and θ' are the angles between the principal axis c of crystal symmetry and the vectors **M**, **M′**; φ and φ' are the azimuthal angles of **M** and **M′** in the basal plane. The term κ**MM′** is the portion of the exchange energy that depends only on the relative orientations of the two sublattices. This portion will be assumed much smaller than the exchange interaction within each of the sublattices; M and M′ can therefore be taken as constant in first approximation. The assumption appears to be a realistic one for the investi-

[1)]Additional curves corresponding to a field parallel to the c axis are omitted to avoid overcrowding the figure.

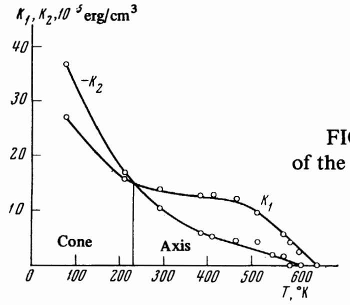

FIG. 2. Temperature dependences of the anisotropy constants K_1 and K_2.

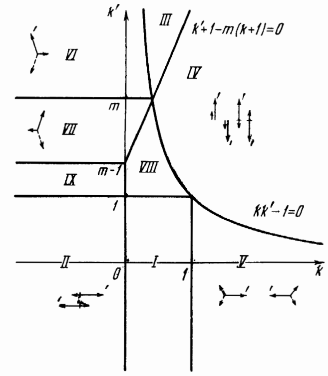

FIG. 3. Plane of the variables k and k′ when k″ = 0 (m = 2.5).

gated ferrites. The last two terms in (2) represent the interaction energy of the crystal and an applied magnetic field **H**.

It is easily seen that a minimum value of (2) can exist when the angles φ, φ' equal 0 or π. We shall therefore confine ourselves henceforth to the xz plane; the z axis coincides with the c axis of the crystal and the x axis coincides with the projection of **H** on the basal plane. The angles φ and φ' can be deleted in (2), while θ and θ' are taken as positive (when $\varphi = 0$) or as negative (when $\varphi = \pi$), having the range 0 to π or 0 to $-\pi$, respectively. We observe that the exchange term $\kappa \mathbf{MM'}$ has the same form as the anisotropy energy terms with K'' and K'''. Therefore $\kappa \mathbf{MM'}$ can be dropped from (2) if we assume that this constant exchange energy is included in the coefficients K'' and K'''. For additional convenience all terms in (2) are normalized to the coefficient K'''.[2)] Equation (2) can now be written as

$$\phi = -\tfrac{1}{2}k\cos^2\theta - \tfrac{1}{2}k'\cos^2\theta' + k''\cos\theta\cos\theta' + \sin\theta\sin\theta' - h_x(\sin\theta + m\sin\theta') - h_z(\cos\theta + m\cos\theta'), \tag{3}$$

where

$$\phi = \frac{\Phi}{K'''}, \quad k = \frac{K}{K'''}, \quad h = \frac{HM}{K'''}, \quad m = \frac{M'}{M}. \tag{4}$$

Since we are interested mainly in ferrimagnetic and antiferromagnetic states rather than ferromagnetic states, we shall assume $K''' > 0$. The conditions $\partial\phi/\partial\theta = 0$ and $\partial\phi/\partial\theta' = 0$ lead to the equations

$$k\cos\theta\sin\theta - k''\sin\theta\cos\theta' + \cos\theta\sin\theta' - h_x\cos\theta + h_z\sin\theta = 0,$$

$$k'\cos\theta'\sin\theta' - k''\sin\theta'\cos\theta + \cos\theta'\sin\theta - h_x m\cos\theta' + h_z m\sin\theta' = 0. \tag{5}$$

The solutions of this system that correspond to the minimum of the thermodynamic potential (3) are derived by analyzing the second derivatives of ϕ.

General analytic solutions of (5) cannot be obtained, but analytic solutions are obtainable in the special case $k'' = 0$ for a field along the x axis. The experimental curves in Fig. 1 show that the solutions for $h = h_x$ are of principal interest. We therefore first consider the case $k'' = 0$, after which we shall investigate the differences that arise when $k'' \neq 0$.

For a zero external field h = 0 we obtain the following stable solutions of (5), corresponding to the absolute minimum of ϕ. In regions I and II (Fig. 3, where $m > 2$) there are two solutions with antiparallel **M** and **M′** along the x axis: $\theta' = -\theta = \pm\pi/2$. In regions III and IV there are four solutions, two with parallel and two with antiparallel orientations of **M** and **M′** along the z axis: $\theta' = \theta = 0, \pi$ and $\theta' = -\theta = 0, \pi$. In region V there are four solutions with **M′** along the x axis and forming an obtuse angle with **M**: $\theta' = \pm\pi/2$, $\sin\theta = \mp 1/k$. In regions VI–IX there are four analogous solutions with **M** and **M′** interchanged: $\theta = \mp\pi/2$, $\sin\theta' = \pm 1/k'$. The fact that in each region there exist several different but equally stable solutions signifies that the crystal can be divided into domains.

If we now refrain from assuming $k'' = 0$, the general character and the number of solutions for h = 0 are not altered. Changes occur with regard to the stable solution regions in the k-k′ plane. For example, the stability boundary of the solutions $\theta' = -\theta = \pm\pi/2$ will be the curve $(k-1)(k'-1) - k''^2 = 0$ (which for $k'' = 0$ degenerates into the two straight lines $k = 1$ and $k' = 1$, as in Fig. 3). The stability boundary of the solutions $\theta' = -\theta = 0, \pi$ will be the curve $(k + k'')(k' + k'') - 1 = 0$. The ferromagnetic solutions $\theta' = \theta = 0, \pi$ become metastable (for $k'' > 0$) and their relative stability boundary runs along the curve $(k - k'')(k' - k'') - 1 = 0$. Similarly, for the ferromagnetic solutions $\theta' = \theta = \pm\pi/2$, which have not been presented here previously because they are metastable (for $k'' \geq 0$), the relative stability boundary runs along the curve $(k+1)(k'+1) - k''^2 = 0$.

We shall now obtain analytic solutions of (5) for $h \neq 0$; it has already been mentioned that this can be done for $h = h_x$. It is here sufficient to limit ourselves to the case of $h_x > 0$ and $m > 1$ (for $m < 1$ the roles of the M and M′ sublattices are interchanged). It will be convenient to have the stable solutions of (5) numbered as follows:

$$1)\ \theta' = \theta = \frac{\pi}{2}, \quad 2)\ \theta' = -\theta = \frac{\pi}{2}, \quad 3)\ \theta' = \frac{\pi}{2},\ \sin\theta = \frac{h-1}{k},$$

$$4)\ \theta = \frac{\pi}{2},\ \sin\theta' = \frac{mh-1}{k'}, \quad 4')\ \theta = -\frac{\pi}{2},\ \sin\theta' = \frac{mh+1}{k'},$$

$$5)\ \sin\theta = \frac{(k'-m)h}{kk'-1}, \quad \sin\theta' = \frac{(km-1)h}{kk'-1}. \tag{6}$$

The following solutions, which are analogous to 1), 2), and 3), are metastable (for $h_x > 0$, $m > 1$) and may be neglected:

[2)]Normalization to K'' (instead of K''') would affect the subsequent analysis only by interchanging the roles of the x and z axes.

$$1')\ \theta' = \theta = -\frac{\pi}{2}, \quad 2')\ \theta' = -\theta = -\frac{\pi}{2},$$
$$3')\ \theta' = -\frac{\pi}{2}, \quad \sin\theta = \frac{h+1}{k} \qquad (7)$$

By investigating the stability of the enumerated solutions we can obtain magnetization curves, i.e., the dependences of the magnetization $I_x = M\sin\theta + M'\sin\theta'$ along the x axis on the applied magnetic field $H = H_x$. These curves are shown in Fig. 4, where $h = h_x$ of Eq. (4) is measured along the horizontal axis and $i = I_x/M$ is measured along the vertical axis. The Roman numerals below the individual graphs correspond to the regions in Fig. 3. The critical fields and the associated magnetizations are shown. The numerals adjacent to the curves denote solutions listed in (6). The dashed lines are metastable states; Fig. 4 does not include the solutions that are given in (7). The existence of metastable solutions permits hysteresis in some instances.

We note that the magnetization curves in Fig. 4 were obtained on the basis of certain assumptions. The omission of a demagnetizing factor means that the results are valid for an infinite crystal. The domain structure of the crystal was neglected; this is equivalent to the assumption that even the weakest possible field produces a single domain. We also neglected the paraprocess, i.e., the change in the absolute magnetic moments M and M′ of the sublattices during the magnetization process.

By now taking k″ into account we do not alter the general character of the magnetization curves in Fig. 4. Changes will occur in the boundaries of the regions of Fig. 3 that enclose some form of each curve. All straight lines in Fig. 4, except the horizontal straight lines representing solutions 1) and 2), will become higher-order curves (see the experimental curves in Fig. 1).

Analytic solutions for the magnetization curves along the z axis cannot be derived even when $k'' = 0$. However, a general analysis reveals that in the most interesting regions (I and II) of Fig. 3 the $I_z(H_z)$ curves will be of the type shown in III, IV of Fig. 4, except that the straight line segments will be replaced by higher-order curves (even when $k'' = 0$).

It is of decided interest to compare the proposed scheme with experiments performed to determine the easy magnetization axis and the anisotropy constants K_1 and K_2. Fields of ~20 kOe were used in the experimental work. It can be assumed that the magnetic vectors of both sublattices were aligned along these fields. The magnetic anisotropy energy can thus be represented by (1), which includes second-order perturbation terms. From a comparison with (2), where we now insert $\theta' = \theta = \psi$, we obtain $K_1 = K + K' - 2(K'' + \kappa MM') + 2(K''' + \kappa MM')$. Figure 2 shows the experimental temperature dependences of K_1 and K_2. We find $K_1 > 0$ in the entire temperature range; this result is consistent with the already observed agreement between the experimental magnetization curve and the theoretical curve of magnetization along the x axis in region I. Agreement

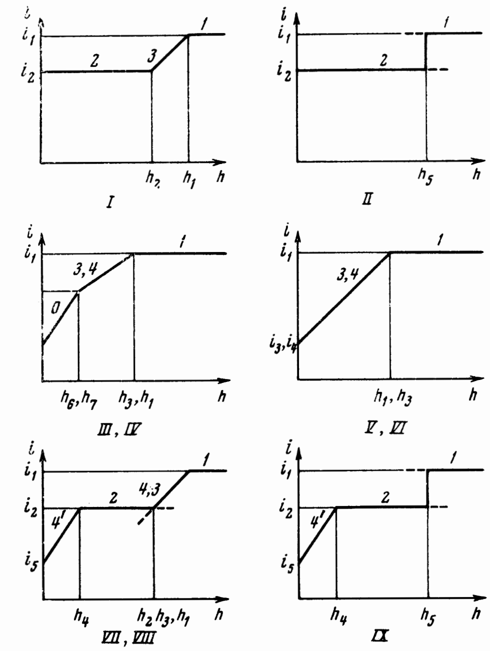

FIG. 4. Magnetization curves for the different regions of the k-k′ plane in Fig. 3; $i = I_x/M$, $h = h_x = h_x M/K'''$. [$h_1 = 1 + k$, $h_2 = 1 - k$, $h_3 = (k' + 1)/m$, $h_4 = (k' - 1)/m$, $h_5 = 1$, $h_6 = (kk' - 1)/(k' - m)$, $h_7 = (kk' - 1)/(mk - 1)$, $i_1 = m + 1$, $i_2 = m - 1$, $i_3 = m - 1/k$, $i_4 = 1 - m/k'$, $i_5 = m/k' - 1$].

was found for $K'' + \kappa MM' = 0$, $K''' + \kappa MM' > 0$, $K > 0$, $K' < 1$.

The curves in Fig. 2 show that the second anisotropy constant K_2, which was neglected in the foregoing theoretical treatment, becomes important below 230°K. If we now attempt in Eq. (2) to take into account terms of the next approximation in the anisotropy energy, an analysis shows that the total number of solutions will be increased. Great diversity of the magnetization curves appears. However, in some regions of the variables k, k′, k″ the previous curves are conserved, especially in regions I and II; these are curves that agree well with experiment. Thus, even when K_2 is taken into account the previous agreement will be obtained, although there will be changes in the regions where the curves of I and II exist. Also, the straight lines become higher-order curves (as occurred when k″ was taken into account).

[1] J. Smit and H. P. J. Wijn, Ferrites, Wiley, New York, 1959 (Russ. transl., IIL, Moscow, 1962).

[2] L. Néel, Izv. Akad. Nauk SSSR, ser. fiz. 21, 890 (1957) [Bull. Acad. Sci. USSR, Phys. Ser. 21, 889 (1957)].

Translated by I. Emin
88